Neuroradiology (2013) 55:853–859
DOI 10.1007/s00234-013-1185-2

DIAGNOSTIC NEURORADIOLOGY

Detection of irreversible changes in susceptibility-weighted images after whole-brain irradiation of children

S. Peters · R. Pahl · A. Claviez · O. Jansen

Received: 22 December 2012 / Accepted: 29 March 2013 / Published online: 16 April 2013

Abstract
Introduction Whole-brain irradiation is part of the therapy protocol for patients with medulloblastomas. Side effects and complications of radiation can be detected by follow-up magnetic resonance imaging (MRI). Susceptibility-weighted images (SWI) can detect even very small amounts of residual blood that cannot be shown with conventional MRI. The purpose of this study was to determine when and where SWI lesions appear after whole-brain irradiation.
Methods MRI follow-up of seven patients with medulloblastoma who were treated with whole-brain irradiation were analyzed retrospectively. SWI were part of the initial and follow-up MRI protocol. De novo SWI lesions, localization, and development over time were documented.
Results At time of irradiation, mean age of the patients was 13 years (±4 years). Earliest SWI lesions were detected 4 months after radiation treatment. In all patients, SWI lesions accumulated over time, although the individual number of SWI lesions varied. No specific dissemination of SWI lesions was observed.
Conclusion Whole-brain irradiation can cause relatively early dot-like SWI lesions. The lesions are irreversible and accumulate over time. Histopathological correlation and clinical impact of these SWI lesions should be investigated.

S. Peters (✉) · O. Jansen
Institute of Neuroradiology, University of Schleswig-Holstein,
Arnold-Heller-Straße 3-Haus 41, Campus Kiel,
24105 Kiel, Germany
e-mail: s.peters@neurorad.uni-kiel.de

R. Pahl
Clinic for Radiooncology, University of Schleswig-Holstein,
Campus Kiel, Kiel, Germany

A. Claviez
Clinic for Paediatrics, University of Schleswig-Holstein,
Campus Kiel, Kiel, Germany

Keywords SWI · Medulloblastom · Irradiation · Pediatrics

Abbreviations
SWI Susceptibility weighted imaging
WHO World Health Organization

Introduction

At a rate of 20 % of all central nervous system tumors in children, medulloblastomas represent the most common malignant (WHO grade IV) brain tumor [1]. The incidence of medulloblastomas in North America is 5 per 1,000,000 in the age range of 0–19 years with a slight male dominance [2]. Owing to the high degree of occult metastasis in the cerebrospinal fluid, whole-brain irradiation constitutes part of the postoperative treatment protocol [3]. The radiation dose varies between 23.4 and 36 Gy, depending on the clinical risk stratification [4–6]. Tumor localization in the posterior fossa receives an additional boost to a total dose of 54–55.8 Gy [4, 6].

Survival rates for patients with meduloblastoma reported in the literature after 5 years are about 70 % [3, 7, 8]. Even 5- and 10-year survival rates of up to 90 % have been described under specific low-risk circumstances [9, 10]. Considering the relatively young age of patients with medulloblastomas and the high survival rates, therapy-related long-term complications in particular need to be minimized. Secondary neoplasms are reported to develop in 4 % of the survivors after 10 years [10]. Other reported complications include neurological and neuropsychological dysfunction, endocrine complications, social impairment, spinal deformities, and alopecia [1, 11].

Late tumor treatment side effects in the brain, which can be detected by magnetic resonance imaging (MRI), are secondary neoplasm, volume loss, and leukencephalopathy

[12]. Additionally, case reports have identified hypointense, dot-like lesions in the radiation fields on T2*-weighted images and susceptibility weighted imaging (SWI) years after the radiation treatment [13, 14].

SWI are ideal for detecting small veins and residual blood in microhemorrhages which cannot be seen on conventional MRI [15–17]. The susceptibility for deoxyhemoglobin, hemosiderin, and ferritin is different from that in the surrounding tissue of the brain. Magnetic susceptibility describes the magnetization of a material in a magnetic field, which depends on the strength of the external magnetic field and the material characteristics [18]. The difference in susceptibility of residual blood leads to a slight local inhomogeneity of the magnetic field, which can be visualized in SWI [15, 18].

The aim of this study was to evaluate whether SWI lesions can be detected in patients with medulloblastoma who received whole-brain radiation treatment. Furthermore, we wanted to determine when and where SWI lesions appear and how they change over time.

Methods

The hospital database was screened for patients in whom uniform whole-brain radiation therapy was given after surgery for medulloblastoma. From 2007 to 2011, eight patients treated for medulloblastoma were identified. One patient succumbed to the disease and there was no follow-up. For the remaining seven patients, the follow-up MRI examinations were reviewed retrospectively.

The MRI examinations were performed on a 3T MRI scanner (Achieva, Phillips Medical Systems, Eindhoven) with an eight-channel head coil. The institutional follow-up protocol for medulloblastomas contains a DWI sequence, an axial T2-weighted sequence, a sagittal FLAIR sequence, an axial SWI sequence, and axial and coronal T1-weighted sequences before and after intravenous administration of a gadolinium-containing contrast agent. The parameters for the 3D SWI sequence were TR=15 ms, TE=21 ms, flip angle=10°, FOV=81 mm, and matrix=220×182. The acquired SWI had a slice thickness of 1 mm. An additional minimum intensity projection was created with a slice thickness of 10 mm. The SWI used by Philips is a PRESTO sequence (principles of echo shifting with a train of observations) where additional field gradients shift the refocused gradient echo into the subsequent TR periods, this results in a TE longer than the TR [19, 20].

For each follow-up MRI, the supratentorial SWI lesions were counted and compared with the previous MRI. The images of each patient where analyzed in chronologic order but the time of radiation was not evident. Lesions were counted manually by one radiologist. To minimize counting bias, the lesions were counted separately for different localizations and each scan was analyzed twice. The localizations of the lesions were distinguished as frontal, parietal, occipital, and temporal. In cases of different counting results for a region, lesions were counted a third time to verify their number. If counting results differ again, an average of all three counts was taken. SWI lesions visible on T1- or T2-weighted images were named macrolesion.

Results

For each patient, six examinations (ranging from five to eight examinations) were reviewed on average. The earliest MRI examination was performed 4 months after the end of whole-brain irradiation. The latest analyzed MRI had been performed 62 months after radiation therapy. The median MRI follow-up time after whole-brain irradiation was 21 months.

All medulloblastoma patients who were followed up with MRI-developed SWI lesions at some point; none of the patients had a leukencephalopathy or radiation necrosis. The earliest SWI lesion was detected 4 months after radiation therapy. This lesion was located in the temporal lobe and the patient had received whole-brain irradiation with a dose of 23.4 Gy. The highest number of 80 lesions was found in a patient treated with whole-brain irradiation at a dose of 35.2 Gy. The radiation treatment had been performed 62 months before MRI (Fig. 1). The lowest number of SWI lesions was found in the occipital lobe; otherwise no specific distribution of SWI lesions was noted.

The number of SWI lesions increased almost linear over time in all patients (Fig. 2). In average, there was a gain of 0.6 lesions per month. However, the number and the gain of lesions varied among the individual patients. Once a lesion appeared, it could be detected during all follow-up examinations (Fig. 3).

Macroscopic lesions that were also visible on T1- or T2-weighted images were detected in four patients. One patient had two such lesions; the rest of the patients had only one macroscopic lesion. The earliest macroscopic lesion was detected 12 months after the end of the irradiation. In two cases, the macroscopic lesion appeared during the follow-up period. In both of these cases, a microscopic SWI lesion was visible in the area of the macroscopic lesion in previous images (Fig. 4).

At the time of radiation therapy, the patients had an average age of 13 years (standard deviation, 4 years; ranging from 8 to 18 years). All patients were treated according to the protocols of a controlled clinical trial (HIT 2000 trial). The average whole-brain radiation dose was 29.5 Gy (standard deviation, 7.2 Gy; ranging from 23.4 to 40 Gy). The uniform whole-brain radiation was applied in fraction; in all

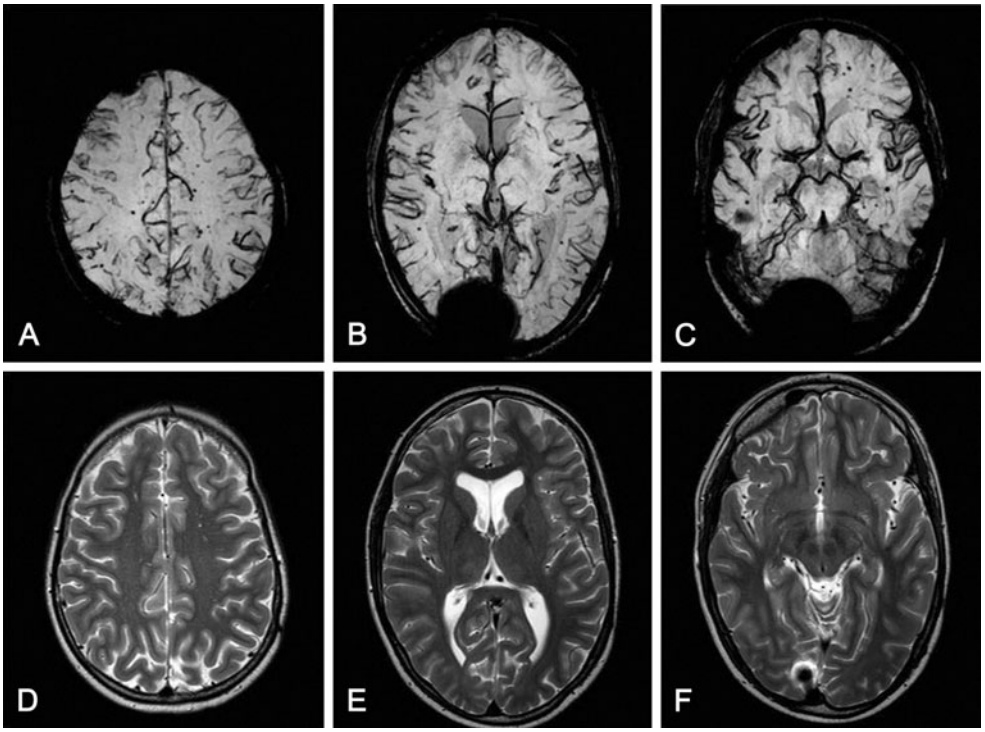

Fig. 1 MRI of a medulloblastoma patient 62 months after whole-brain irradiation with a dose of 35.2 Gy. Multiple dot-like lesions are shown in the SWI in all lobes (**a**–**c**). The occipital signal alterations are caused by postoperative skull fixation. None of those lesions are visible in T2-weighted images (**d**–**f**). The patient was 11 years at the time of radiation treatment

patients, the infratentorial tumor localization received a boost. Additionally, all patients received systemic chemotherapy.

No correlation was found between the number of SWI lesions and the radiation dose or the patient age at the time of radiotherapy in this study. Further, no correlation between the gain of SWI lesions over time and the age or dose was found.

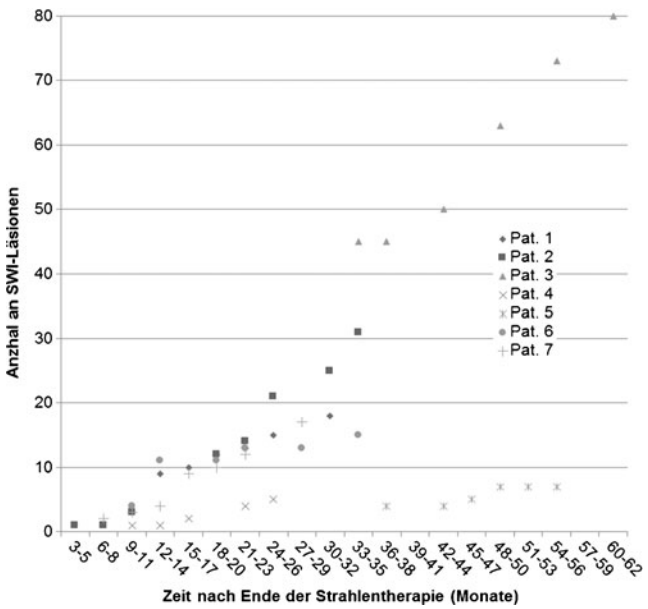

Fig. 2 Number of dot-like hypointense lesions in SWI in relation to the time since completing the radiation therapy. The number of lesions increased in an almost linear fashion over time, although the individual lesion count varies

Discussion

In contrast to other patients with solitary primary brain tumors, medulloblastoma patients receive whole-brain irradiation in addition to local radiation treatment of the tumor bed. Considering the young age of medulloblastoma patients and the relatively high survival rates, the possible long-term complications of whole-brain irradiation need to be minimized.

This study shows clearly that small hypointense lesions can be detected by MRI using SWI while no changes are seen in these areas in conventional MRI. Cases of dot-like lesions on SWI or T2*-weighted images have been reported before; however, the lesions were detected years after irradiation in these reports [13, 14]. In adults, the earliest lesion was reported 2 years after the radiation [13]. Our study shows that such lesions can develop much sooner in irradiated children. The first lesion we detected with SWI had already developed 4 months after radiation treatment.

Although a correlation between lesion count and time has already been reported [13], these reports were cross-sectional in nature and did not include serial data from an individual patient. With our approach, we also attempted to analyze the intraindividual dynamics of the lesion burden. In this study, the SWI lesions accumulated in an almost linear

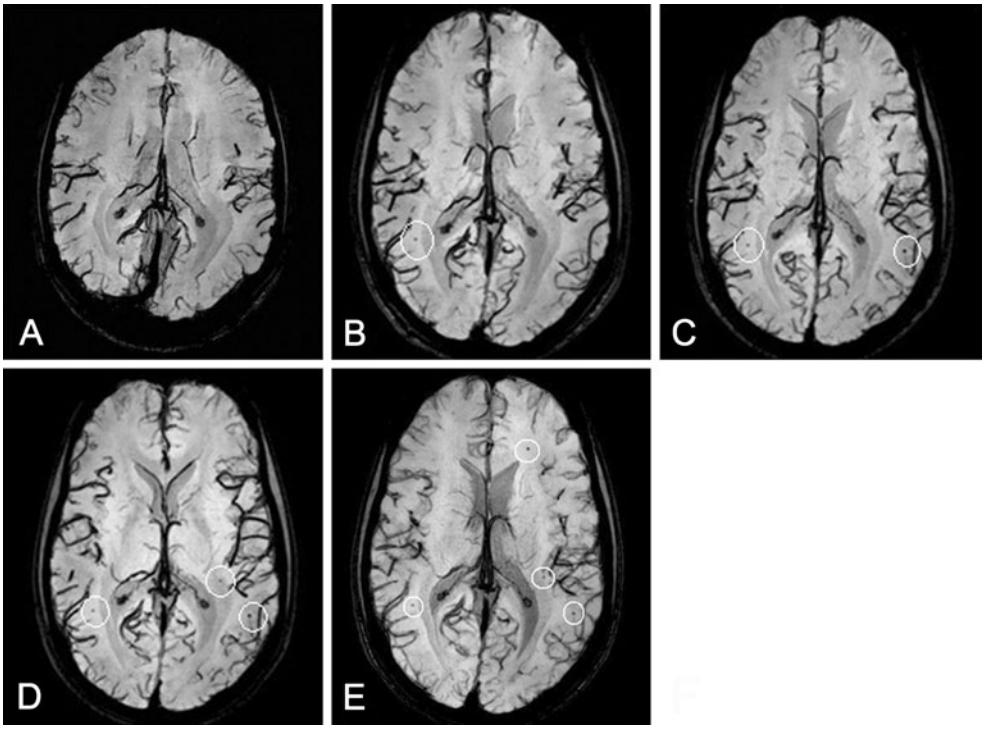

Fig. 3 SWI of a medulloblastoma patient who had received whole-brain radiation therapy with a dose of 23.4 Gy at the age of 16 years. The images were acquired 10 months (**a**), 20 months (**b**), 26 months (**c**), 30 months (**d**), and 33 months (**e**) after the end of the radiation treatment. The hypodense lesions (*encircled*) accumulate over time and do not disappear. In **a**, SWI lesions are visible in other slices that are not shown here

fashion over time in each patient and once a lesion appeared, it was irreversible. However, the number of lesions varied substantially between patients at similar time points after radiation treatment. Furthermore, the gain in lesions per time period varies between the patients. Given that no correlation of the radiation dose or the patient age was found and all patients received additional chemotherapy, it would appear that the individual vulnerability varies. The risk of developing SWI lesions after whole-brain irradiation in childhood or adolescence seems to be quite high. In our study, all followed up meduloblastoma patients developed new SWI lesions at some point.

It is well known that conventional MRI can show hypointense lesions in T2-weighted images years after

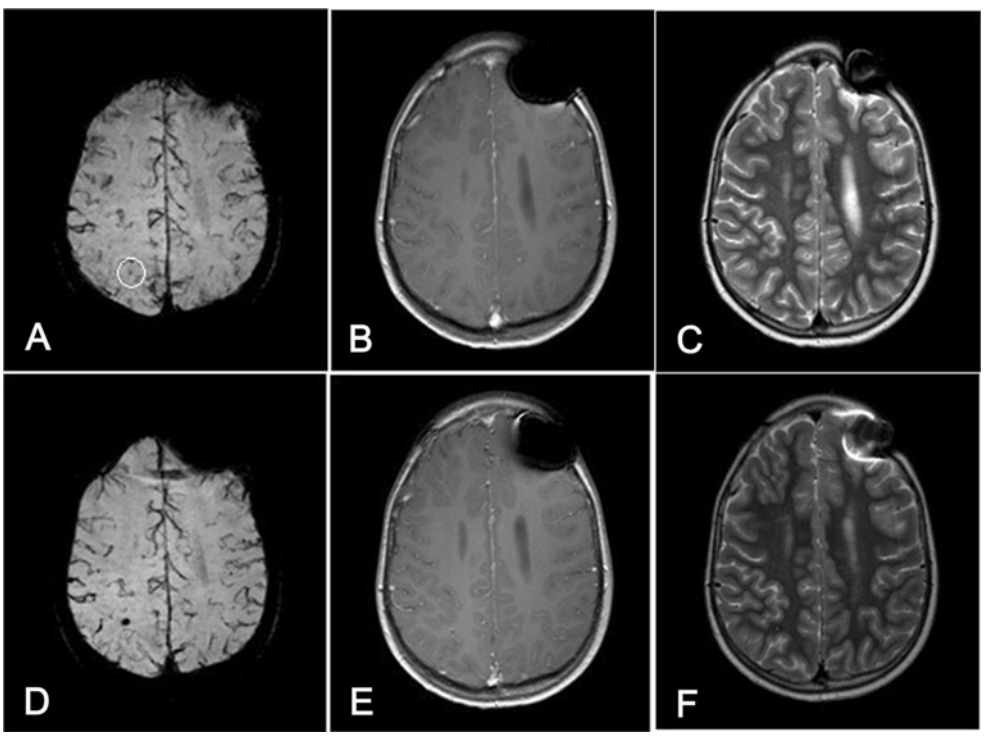

Fig. 4 MRI follow-up of a medulloblastoma patient who had received whole-brain radiation therapy with a dose of 40 Gy. In SWI, 23 months after the radiation a dotlike hypointense lesion is visible in the right parietal lobe (*encircled*; **a**). At this time, the T1- and T2-weighted images show no lesions in this area (**b** and **c**). At the follow-up MRI, 27 months after whole-brain irradiation the SWI lesion is increased in size (**d**) and a lesion is visible on T1- and T2-weighted images (**e** and **f**). The patient had more SWI lesions that are not shown in these slices. Left frontal signal alterations are due to a ventricular puncture system

radiation therapy. In most cases, they are called radiation-induced cavernomas or radiation-induced telangiectasias [21–29]. The name is based on their similarity to cavernomas on MRI and CT. Overall, incidence ranges between 3.4 and 20 % [24, 27, 29]. Clinical complications such as bleeding or seizures have only been described in rare cases. The histological evaluation of these bleedings, if they are treated surgically, is described as "consistent with cavernoma" [21, 30]. Cavernomas can be stable in size, grow, or even shrink [21, 25, 31]. In this study, we were able to observe very small lesions that can only be demonstrated with these very sensitive SWI sequences. We even observed single SWI lesions that increased in size to lesions that can be detected on conventional MRI during follow-up. We speculate that the so-called radiation-induced cavernomas visible in conventional MRI are only the *tip of the iceberg*, although it seems unlikely that all SWI lesions grow to lesions visible in conventional MRI. The majority of SWI lesions will never be visible in conventional MRI.

The correlation of radiation-induced cavernomas with patient age or radiation dose is the subject of discussion and some authors state that more cavernomas are associated with younger age at therapy and with higher radiation doses [21, 23–27, 29]. In this study, a trend was observed for detecting cavernomas on conventional MRI with increased number of SWI lesion, irrespective of age or radiation dose. Due to the limited patient number and the retrospective character of the study, a reliable statistical conclusion cannot be made. Furthermore, all of our study patients were under the age of 20 years and the radiation dose ranged from 23.4 to 40 Gy. For both the age and the dose, the dispersion is small so that an existing correlation might be missed. An effect of age for example might be evident by comparing adults to children and adolescents.

The described increased vulnerability for developing radiation-induced lesions of the temporal lobes [25] could not be confirmed. Apart from fewer lesions in the occipital lobe, our study did not detect any distinct distribution of lesion number or lesion location. However, the lobes where not normalized by volume, which complicates a direct comparison. The lower number of occipital SWI lesions might be explained by the smaller size of the occipital lobe and not be obvious after normalizing the volumes. As mentioned before, we tried to minimize the counting bias by analyzing the images twice and separate for the lobes; nevertheless, an uncertainty of detection accuracy remains. The infratentorial parts of the brain were deliberately not analyzed. Owing to the location of medulloblastomas near the fourth ventricle, operation and radiation boost in this area cannot be adequately compared with the other parts of the brain. Confounding artifacts from postoperative metallic hardware or blood products might lead to biases. Further, the caudal parts of the cerebellum are at the edge of the brain volume scanned with SWI and therefore are only captured variably and incompletely in some cases.

We still have not identified a histological correlate of SWI lesions. Histological studies on rats that underwent brain irradiation found vessel dilatations and thickening of the vessel walls. Degeneration of smooth muscle cells in arterioles and fibrin deposition in dilated capillary walls was also described [32–35]. The rats were irradiated once, and therefore the radiation settings differed considerably from the radiation in tumor therapy where the dose is fractionated. Radiation with fractions of a lower dose induces different tissue reactions. In rats irradiated with a fractionated dose, a decrease in vessel density has been described [36]. Furthermore, human and rat brains show a different sensitivity to irradiation [37]. For these reasons, findings gained from animal studies cannot be directly compared to humans. Histological studies in humans are only conducted in cases of hemorrhage and operation. In these rarely reported cases, thin-walled vessels surrounded by hemosiderin and intramural fibrin were found [38, 39]. However, no data exist concerning histological examinations of parts of the brain outside the hemorrhagic area.

There are different reasons for hypointense lesions in SWI. As previously described, iron-containing blood products such as deoxyhemoglobin, hemosiderin, and ferritin can cause such lesions [15, 18]. In oxygenated hemoglobin, the iron is shielded by the oxygen so that small arterial vessels cannot be seen [16, 18]. Calcium is another substance that generates SWI lesions [18]. Considering the results of the animal experiments and the rare histological findings in humans, it seems likely that the SWI lesions are small venous telangiaectasias or microhemorrhages.

Another point is the uncertain clinical relevance of the SWI lesions. As shown in our study, single of these small SWI lesions might grow in size and become visible on conventional MRI. Fortunately, these so-called radiation-induced cavernomas are mostly clinically asymptomatic [21, 24, 25]. In some cases, they might bleed and cause seizures or headache. Only patients who develop such symptoms might require surgery; otherwise, no therapy is necessary [21, 24–27, 29, 30].

Multiple SWI lesions are also observed in patients with cerebral amyloid angiopathy [17, 40–43]. These lesions look similar to radiation-induced SWI lesions and they even show a similar distribution. Histologically, confirmed causes for the SWI lesions in patients with cerebral amyloid angiopathy are microbleeds, extravasated blood, and hemosiderin. β-amyloid was found in the vessel walls near the hemorrhages [42]. The number of lesions correlates negatively with the cognitive performance of these individuals [44]. Whereas cognitive impairment is a well-known and

described complication of cerebral irradiation, this might also correlate with the number of SWI lesions in medulloblastoma patients as described for cerebral amyloid angiopathy.

Conclusion

After whole-brain irradiation, hypointense, dot-like lesions can be detected with SWI. The SWI lesions are irreversible and accumulate in an almost linear fashion over time. No specific distribution of these lesions could be found. A few lesions can even grow in size and be identified on conventional MRI; however, this is not the case for the majority of SWI lesions. The histopathological correlation is not clear and the clinical relevance remains uncertain, too.

Conflict of interest We declare that we have no conflict of interest.

References

1. Frühwald MC, Rutkowski S (2011) Tumors of the central nervous system in children and adolescents. Dtsch Arztebl 108(22):390–397
2. Kohler BA, Ward E, McCarthy BJ, Schymura MJ, Ries LAG, Eheman C et al (2011) Annual report to the nation on the status of cancer, 1975–2007, featuring tumors of the brain and other nervous system. J Natl Cancer Inst 103(9):714–736
3. Kortmann RD, Kühl J, Timmermann B, Mittler U, Urban C, Budach V et al (2000) Postoperative neoadjuvant chemotherapy before radiotherapy as compared to immediate radiotherapy followed by maintenance chemotherapy in the treatment of medulloblastoma in childhood: results of the German prospective randomized trial HIT '91. Int J Radiat Oncol Biol Phys 46(2):269–279
4. Ramaswamy V, Northcott PA, Taylor MD (2011) FISH and chips: the recipe for improved prognostication and outcomes for children with medulloblastoma. Cancer Genet 204(11):577–588
5. Khatua S, Sadighi ZS, Pearlman ML, Bochare S, Vats TS (2012) Brain tumors in children—current therapies and newer directions. Indian J Pediatr 79(7):922–927
6. Pollack IF (2011) Multidisciplinary management of childhood brain tumors: a review of outcomes, recent advances, and challenges. J Neurosurg Pediatr 8(2):135–148
7. Rieken S, Mohr A, Habermehl D, Welzel T, Lindel K, Witt O et al (2011) Outcome and prognostic factors of radiation therapy for medulloblastoma. Int J Radiat Oncol Biol Phys 81(3):e7–e13
8. Jakacki RI, Burger PC, Zhou T, Holmes EJ, Kocak M, Onar A et al (2012) Outcome of children with metastatic medulloblastoma treated with carboplatin during craniospinal radiotherapy: a children's oncology group phase I/II study. J Clin Oncol 30(21):2648–2653
9. Packer RJ, Sutton LN, Elterman R, Lange B, Goldwein J, Nicholson HS et al (1994) Outcome for children with medulloblastoma treated with radiation and cisplatin, CCNU, and vincristine chemotherapy. J Neurosurg 81(5):690–698
10. Von Hoff K, Hinkes B, Gerber NU, Deinlein F, Mittler U, Urban C et al (2009) Long-term outcome and clinical prognostic factors in children with medulloblastoma treated in the prospective randomised multicentre trial HIT'91. Eur J Cancer 45(7):1209–1217
11. Frange P, Alapetite C, Gaboriaud G, Bours D, Zucker JM, Zerah M et al (2009) From childhood to adulthood: long-term outcome of medulloblastoma patients. The Institut Curie experience (1980–2000). J Neurooncol 95(2):271–279
12. Vázquez E, Delgado I, Sánchez-Montañez A, Barber I, Sánchez-Toledo J, Enríquez G (2011) Side effects of oncologic therapies in the pediatric central nervous system: update on neuroimaging findings. Radiographics 31(4):1123–1139
13. Lupo JM, Chuang CF, Chang SM, Barani IJ, Jimenez B, Hess CP et al (2012) 7-Tesla susceptibility-weighted imaging to assess the effects of radiotherapy on normal-appearing brain in patients with glioma. Int J Radiat Oncol Biol Phys 82(3):e493–e500
14. Noyce AJ, McCrae S, Gawler J, Evanson J (2010) Teaching neuroimages: microhemorrhages resulting from cranial radiotherapy in childhood. Neurology 75(1):e2–e3
15. Rauscher A, Sedlacik J, Deistung A, Mentzel H-J, Reichenbach JR (2006) Susceptibility weighted imaging: data acquisition, image reconstruction and clinical applications. Z Med Phys 16(4):240–250
16. Sehgal V, Delproposto Z, Haddar D, Haacke EM, Sloan AE, Zamorano LJ et al (2006) Susceptibility-weighted imaging to visualize blood products and improve tumor contrast in the study of brain masses. J Magn Reson Imaging 24(1):41–51
17. Mittal S, Wu Z, Neelavalli J, Haacke EM (2009) Susceptibility-weighted imaging: technical aspects and clinical applications, part 2. AJNR Am J Neuroradiol 30(2):232–252
18. Haacke EM, Mittal S, Wu Z, Neelavalli J, Cheng Y-CN (2009) Susceptibility-weighted imaging: technical aspects and clinical applications, part 1. AJNR 30(1):19–30
19. Tsuboyama T, Imaoka I, Shimono T, Nakatsuka T, Ashikaga R, Okuaki T et al (2008) T2*-sensitized high-resolution magnetic resonance venography using 3D-PRESTO technique. Magn Reson Med Sci 7(2):73–77
20. Moonen CT, Liu G, Van Gelderen P, Sobering G (1992) A fast gradient-recalled MRI technique with increased sensitivity to dynamic susceptibility effects. Magn Reson Med 26(1):184–189
21. Lew SM, Morgan JN, Psaty E, Lefton DR, Allen JC, Abbott R (2006) Cumulative incidence of radiation-induced cavernomas in long-term survivors of medulloblastoma. J Neurosurg 104(2 Suppl):103–107
22. Jain R, Robertson PL, Gandhi D, Gujar SK, Muraszko KM, Gebarski S (2005) Radiation-induced cavernomas of the brain. AJNR Am J Neuroradiol 26(5):1158–1162
23. Vinchon M, Leblond P, Caron S, Delestret I, Baroncini M, Coche B (2011) Radiation-induced tumors in children irradiated for brain tumor: a longitudinal study. Childs Nerv Syst 27(3):445–453
24. Koike S, Aida N, Hata M, Fujita K, Ozawa Y, Inoue T (2004) Asymptomatic radiation-induced telangiectasia in children after cranial irradiation: frequency, latency, and dose relation. Radiology 230(1):93–99
25. Martínez-Lage JF, De la Fuente I, Rosde San Pedro J, Fuster JL, Pérez-Espejo MA, Herrero MT (2008) Cavernomas in children with brain tumors: a late complication of radiotherapy. Neurocirugia (Astur) 19(1):50–54
26. Nimjee SM, Powers CJ, Bulsara KR (2006) Review of the literature on de novo formation of cavernous malformations of the central nervous system after radiation therapy. Neurosurg Focus 21(1):e4
27. Burn S, Gunny R, Phipps K, Gaze M, Hayward R (2007) Incidence of cavernoma development in children after radiotherapy for brain tumors. J Neurosurg 106(5 Suppl):379–383

28. Furuse M, Miyatake S-I, Kuroiwa T (2005) Cavernous malformation after radiation therapy for astrocytoma in adult patients: report of 2 cases. Acta Neurochir 147(10):1097–1101, discussion 1101
29. Strenger V, Sovinz P, Lackner H, Dornbusch HJ, Lingitz H, Eder HG et al (2008) Intracerebral cavernous hemangioma after cranial irradiation in childhood. Incidence and risk factors. Strahlenther Onkol 184(5):276–280
30. Baumgartner JE, Ater JL, Ha CS, Kuttesch JF, Leeds NE, Fuller GN et al (2003) Pathologically proven cavernous angiomas of the brain following radiation therapy for pediatric brain tumors. Pediatr Neurosurg 39(4):201–207
31. Washington CW, McCoy KE, Zipfel GJ (2010) Update on the natural history of cavernous malformations and factors predicting aggressive clinical presentation. Neurosurg Focus 29(3):E7
32. Münter MW, Karger CP, Reith W, Schneider HM, Peschke P, Debus J (1999) Delayed vascular injury after single high-dose irradiation in the rat brain: histologic immunohistochemical, and angiographic studies. Radiology 212(2):475–482
33. Kamiryo T, Kassell NF, Thai QA, Lopes MB, Lee KS, Steiner L (1996) Histological changes in the normal rat brain after gamma irradiation. Acta Neurochir 138(4):451–459
34. Reinhold HS, Hopewell JW (1980) Late changes in the architecture of blood vessels of the rat brain after irradiation. Br J Radiol 53(631):693–696
35. Hopewell JW, Calvo W, Campling D, Reinhold HS, Rezvani M, Yeung TK (1989) Effects of radiation on the microvasculature. Implications for normal-tissue damage. Front Radiat Ther Oncol 23:85–95
36. Brown WR, Thore CR, Moody DM, Robbins ME, Wheeler KT (2005) Vascular damage after fractionated whole-brain irradiation in rats. Radiat Res 164(5):662–668
37. Karger CP, Münter MW, Heiland S, Peschke P, Debus J, Hartmann GH (2002) Dose-response curves and tolerance doses for late functional changes in the normal rat brain after stereotactic radiosurgery evaluated by magnetic resonance imaging: influence of end points and follow-up time. Radiat Res 157(6):617–625
38. Gaensler EH, Dillon WP, Edwards MS, Larson DA, Rosenau W, Wilson CB (1994) Radiation-induced telangiectasia in the brain simulates cryptic vascular malformations at MR imaging. Radiology 193(3):629–636
39. Poussaint TY, Siffert J, Barnes PD, Pomeroy SL, Goumnerova LC, Anthony DC et al (1995) Hemorrhagic vasculopathy after treatment of central nervous system neoplasia in childhood: diagnosis and follow-up. AJNR 16(4):693–699
40. Ku H-L, Chi N-F (2011) Cerebral lobar microhemorrhages detection by high magnetic field susceptibility weighted image: a potential diagnostic neuroimage technique of Alzheimer's disease. Med Hypotheses 76(6):840–842
41. Charidimou A, Jäger HR, Werring DJ (2012) Cerebral microbleed detection and mapping: principles, methodological aspects and rationale in vascular dementia. Exp Gerontol 7(11):843–852
42. Schrag M, McAuley G, Pomakian J, Jiffry A, Tung S, Mueller C et al (2010) Correlation of hypointensities in susceptibility-weighted images to tissue histology in dementia patients with cerebral amyloid angiopathy: a postmortem MRI study. Acta Neuropathol 119(3):291–302
43. Werring DJ, Gregoire SM, Cipolotti L (2010) Cerebral microbleeds and vascular cognitive impairment. J Neurol Sci 299(1–2):131–135
44. Poels MMF, Ikram MA, Van der Lugt A, Hofman A, Niessen WJ, Krestin GP et al (2012) Cerebral microbleeds are associated with worse cognitive function: the Rotterdam Scan Study. Neurology 78(5):326–333